CHAPTER II

THEORY AND LITERATURE REVIEW

2.1 Patterned Polymer Film

Artificially designed fine patterning of polymer films have received a great deal of attention in various fields of science and technology such as microelectronics, anti-etching optical devices, biological and chemical sensors, and tissue engineering. Moreover, their relevance as model heterogeneous systems has led to fundamental understanding of interface phenomena. This growing field has produced a variety of surface patterns at both nanometer and micrometer scales. Thin films of polymers that incorporate reactive functional groups provide a surface that can be further modified by chemical reactions. Methods for attaching polymers to self-assembly monolayer (SAMs) have been continuously developed, for example, electrostatic adsorption of polyelectrolytes to an oppositely charged surface, chemisorption of polymers containing reactive groups to a surface, and covalent attachment of polymers to reactive SAMs. At present, there are a few methods available for patterning thin films of polymers on SAMs. These include procedures based on photolithography, templating the deposition of polymers using patterned SAMs, and templating phase separation in diblock copolymers.

Recently, polymer brushes have attracted considerable attention for creating patterned surface because of their novel structures and properties. An assembly patterned polymer brushes could be obtained by traditional photolithography or chemical amplification of patterned SAMs.

In 1997, Rühe and coworkers [1] explored the preparation of patterned, covalently tethered polymer brushes by photolithography using an appropriate mask and deep or near UV irradiation before, during and after polymer brush formation.

Three approaches were attempted. First, surface reactions were carried out to remove tethered polymer chains from selected areas. The second approach used light irradiation to decompose immobilized azo initiators in selected areas followed by polymer brush formation through thermally induced radical polymerization in the unirradiated areas. The third technique was photoactivation of an initiator through a mask leading to photopolymerization in selected areas. All three approaches allowed preparation of patterned, covalently tethered polymer brushes with a high spatial resolution. Using photolithography, in 1997, Chen and coworkers [2] obtained micropatterned, immobilized poly(acrylic acid) on a polystyrene film. In 2000, Hawker and coworkers [3] used TEMPO-mediated radical polymerization to prepare a poly(*tert*-butyl acrylate) brush on a silicate substrate. A polystyrene film containing bis(*tert*-butylphenyl)iodonium triflate was spin-cast onto the polymer brush followed by exposure of the surface to UV radiation through a mask. Photogenerated acid converted poly(*tert*-butyl acrylate) brushes to poly(acrylic acid) brushes. The end result was a patterned surface containing distinct areas of hydrophobic and hydrophilic brushes.

In 1998, Whitesides and coworkers [4] have introduced the concept of microcontact printing (μCP) to prepare patterned SAMs. This method has been extended into patterning polymer films. Later in 1999, they reported patterned polymer growth on silicon surfaces using μCP and surface-initiated polymerization. [5] Microcontact printing was used to prepare a patterned SAM composed of octadecyltrichlorosilane and norbornenyl trichlorosilane. Exposure of the surface to a Ru metathesis catalyst followed by surface-initiated ROMP of norbornene produced patterned polymer brushes. The patterned polymer films were successfully used as reactive ion etching resists. In the same year, Hussemann and coworkers [6] have successfully achieved patterned, covalently tethered polymer brushes by chemical amplification from patterned SAMs with hydroxyl and methyl terminal groups. Their strategy is illustrated in Figure 2.1. Di(ethylene glycol) and methyl-terminated monolayers were patterned by μCP on gold surface. Surface-initiated ring opening polymerization of ∈–carprolactone in the presence of a free initiator such as benzyl

alcohol catalyzed by triethylaluminum under suitable conditions produced tethered polymer brushes in the hydroxyl functionalized areas. It was found that the thickness of poly(∈-carprolactone) varied linearly with the $\overline{M}_n$ of the free polymer formed in solution from the added initiator. In 2000, Shah et al. [7] used ATRP to amplify initiator monolayers prepared by μCP on gold surfaces.

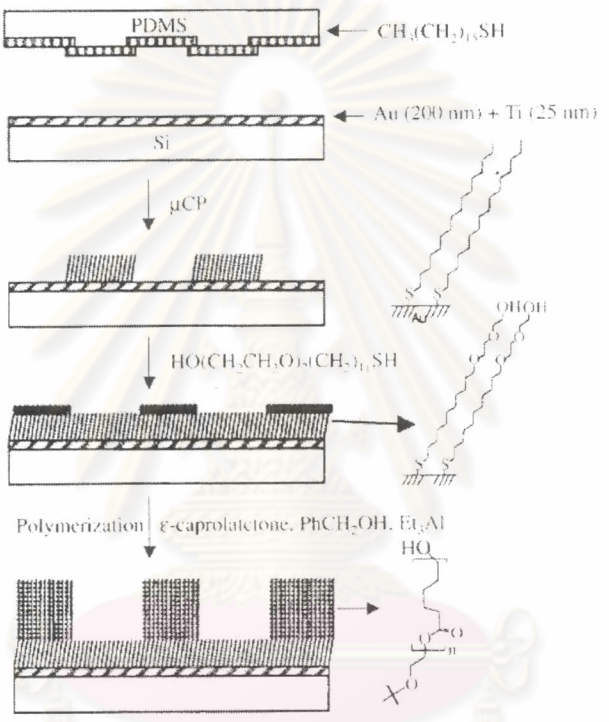

Figure 2.1 Strategy for amplification of a patterned SAM prepared by microcontact printing into a patterned polymer brush.

In 1999, Yan et al. [8] described the patterning of poly(ethylene imine) (PEI) on a surface into structures having submicron edge resolution. These patterned thin films of PEI are attached covalently to the SAM by amide bonds. These procedure consists of 3 steps : (1) formation of a reactive SAM terminating in interchain carboxylic anhydride group on gold and silver; (2) patterning of this SAM by microcontact printing using a poly(dimethylsiloxane) stamp linked with PEI; (3) hydrolysis of the unreacted anhydride groups with base and removal of noncovalently bound PEI.

In the same year, Ingall and coworkers [9] reported a method for the production of patterned monolayers that allows the generation of micron sized features by creating a phenylsilane monolayer on the oxide surface and then using 193 nm light to cleave the surface phenyl groups; the remaining groups can then be functionalized to create surface – grafted patterned polymer layers.

Furthermore, McCarthy and Fadeev [10,11] prepared tris(TMS) monolayers which was used as patterns for the synthesis of uniformly mixed binary monolayers of organosilanes on oxidized silicon wafers. Data from contact angle studies using probe fluids of different sizes suggested that tris(TMS) monolayers have interstitial holes with the size of nanometers (nanopores). Reported Later by McCarthy and coworkers, the controlled over the surface coverage of tris(TMS) was used to manipulate the distribution and size of these nanopores and generated model of chemically heterogeneous surfaces (silanol mixed with tris(TMS)) for adsorption of functionalized polystyrene. Unreacted silanol groups on the substrate surface were used as adsorption sites for carboxylic acid end-functionalized polystyrene (PS-COOH). The thickness of the adsorbed layer could be controlled by the tris(TMS) surface coverage, adsorbing solvent, polymer molecular weight and adsorption time. The thickness of the adsorbed polymer layer decreased with increasing tris(TMS) coverage. An increase in the total adsorbed thickness was evidenced as the molecular weight of the polymer and a number of chains anchored to the surface increased. For the surface topography, the tris(TMS)-modified surface having been adsorbed PS-COOH exhibited texture arising from the incomplete coverage of the surface with tris(TMS). Aggregates of the adsorbed PS-COOH having an average height of 1.2 nm and diameter of 22 nm were also observed. An average separation distance of adsorbed PS-COOH increased with increasing tris(TMS) coverage.

In 2002, Tsujii and coworkers [12] attempted to fabricate a finely patterned graft layer with a nano-scale resolution by the combined use of surface-initiated living radical polymerization and electron beam lithography; the electron beam was scanned on an initiator – immobilized substrate to selectively bombard and decompose the initiator, followed by the electron beam induced pattern, which was amplified by the atom transfer radical polymerization (ATRP). This system

understudy indicated that increasing electron beam doses was required to cope with the relatively low electron beam sensitivity of the initiators, resulting in a decrease in the graft density of the polymer

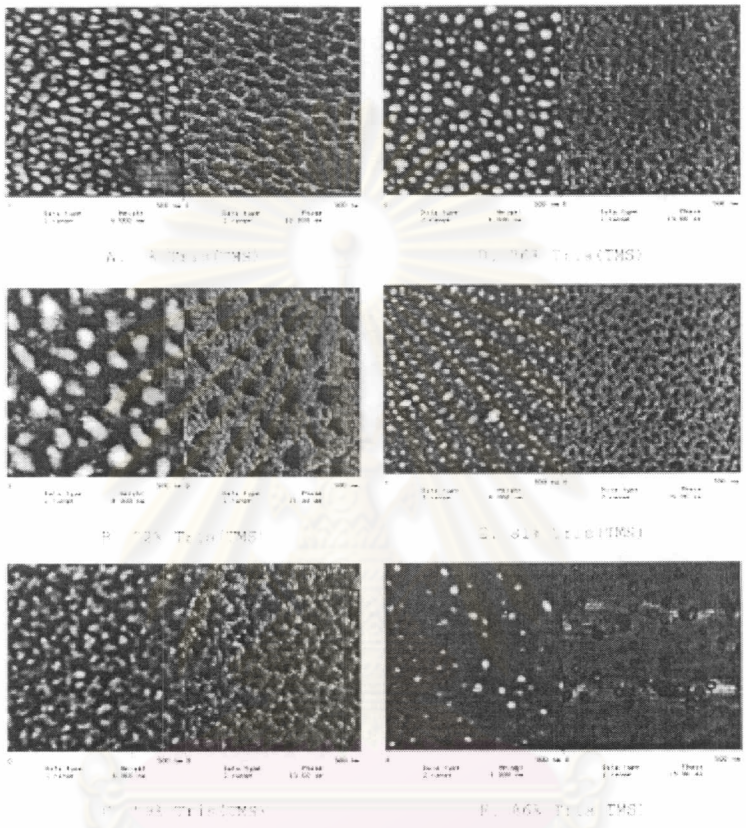

Figure 2.2 AFM images (height/phase) of 11K PS-COOH adsorbed from toluene to tris(TMS) modified surfaces

2.2 Living Polymerization

Synthetic polymers are long-chain molecules possessing uniform repeat units (mers). The chains are not all the same length. These giant molecules are of interest because of their physical properties, in contrast to low molecular weight molecules, which are of interest due to their chemical properties. Possibly the most useful physical property of polymers is their low density versus strength.

When synthetic polymers were first introduced, they were made by free radical initiation of single vinyl monomers or by chemical condensation of small difunctional molecules. The range of their properties was understandably merger. Random copolymers are greatly expanding in the range of useful physical properties such as toughness, hardness, elasticity, compressibility, and strength, however, polymer chemists realized that their materials could not compare with the properties of natural polymers, such as wool, silk, cotton, rubber, tendons, and spider webbing. The natural polymers are generally condensation polymers made by addition of monomer units one at a time to the ends of growing polymer chains. Polymerization of all chains stops at identical molecular weights. For some time polymer chemists have realized that to approach nature's degree of sophistication, new synthetic techniques would be needed.

Conventional chain-growth polymerizations, for example, free radical synthesis, consist of four elementary steps: initiation, propagation, chain transfer, and termination. As early as 1936, Ziegler proposed that anionic polymerization of styrene and butadiene, consecutive addition of monomer to an alkyl lithium initiator occured without chain transfer or termination. During transferless polymerization, the number of polymer molecules remains contant. Since there is no termination, active anionic chain ends remain after all of the monomer has been polymerized. When fresh monomer is added, polymerization resumes. The name "living polymerization" was coined for the method by Szwarc [13], because the chain ends remain active until killed. The term has nothing to do with living in the biological sense. Before Szwarc's classic work, Flory [14] had described the properties associated with living polymerization of ethylene oxide initiated with alkoxides. Flory noted that since all of the chain ends grow at the same rate, the molecular weight is determined by the amount of initiator used versus monomer (Eq. 2.1)

$$\text{Degree of polymerization} = [\text{monomer}]/[\text{initiator}] \qquad (2.1)$$

Another property of polymers produced by living polymerization is the very narrow molecular weight distribution. The polydispersity (D) has a Poisson distribution, $D = \overline{M}_w/\overline{M}_n = 1 + (1/dp)$; $\overline{M}_w$ is the average molecular weight

determined by light scattering, $\overline{M}_n$ is the average molecular weight determined by osmometry, and *dp* is the degree of polymerization (the number of monomer units per chain). The values of $\overline{M}_w$ and $\overline{M}_n$ can also be determined by gel permeation chromatography (GPC). A living polymerization can be distinguished from free radical polymerization or from a condensation polymerization by plotting the molecular weight of the polymer versus conversion. In a living polymerization, the molecular weight is directly proportional to conversion (Figure 2.3, line A). In a free radical or other nonliving polymerization, high molecular weight polymer is formed in the initial stages (line B), and in a condensation polymerization, high molecular weight polymer is formed only as the conversion approaches 100% (line C).

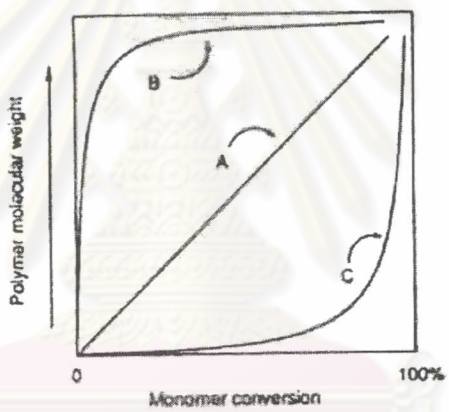

Figure 2.3 Molecular weight conversion curves for various kinds of polymerization methods: (A) living polymerization; (B) free radical polymerization; and (C) condensation polymerization.

Living polymerization techniques give the synthetic chemist two particularly powerful tools for polymer chain design: the synthesis of block copolymers by sequential addition of monomers and the synthesis of functional-ended polymers by selective termination of living ends with appropriate reagents. The main architectural features available starting with these two basic themes are listed in Figure 2.4 along with applications for the various polymer types. Although living polymerization of only a few monomers is nearly perfect, a large number of other systems fit theory close enough to be useful for synthesis of the wide variety of different polymer chain

structures. In general, the well-behaved living systems need only an initiator and monomer, as occurs in the anionic polymerization of styrene, dienes, and ethylene oxide. For an increasing number of monomers, more complex processes are needed to retard chain transfer and termination. These systems use initiators, catalysts, and sometimes chain-end stabilizers. The initiator begins chain growth and in all systems is attached (or part of it, at least) to the nongrowing chain end. The catalyst is necessary for initiation and propagation but is not consumed. The chain-end stabilizer usually decreases the polymerization rate. When the catalyst is a Lewis acid (electron-pair acceptor), the stabilizer will likely be a Lewis base (electron-pair donor), and vice versa. In all systems, the initiation step must be faster than or the same rate as chain propagation to obtain molecular weight control. If the initiation rate is slower than the propagation rate, the first chains formed will be longer than the last chains formed. If an initiator with a structure similar to that of the growing chain is chosen, the initiation rate is assured of being comparable to the propagation rate. A number of living systems operate better if excess monomer is present. A possible explanation is that the living end is stabilized by complexation with monomer [15]. Large counterions tend to be more effective than small counterions in living polymerization systems even when the ionic center is only indirectly involved.

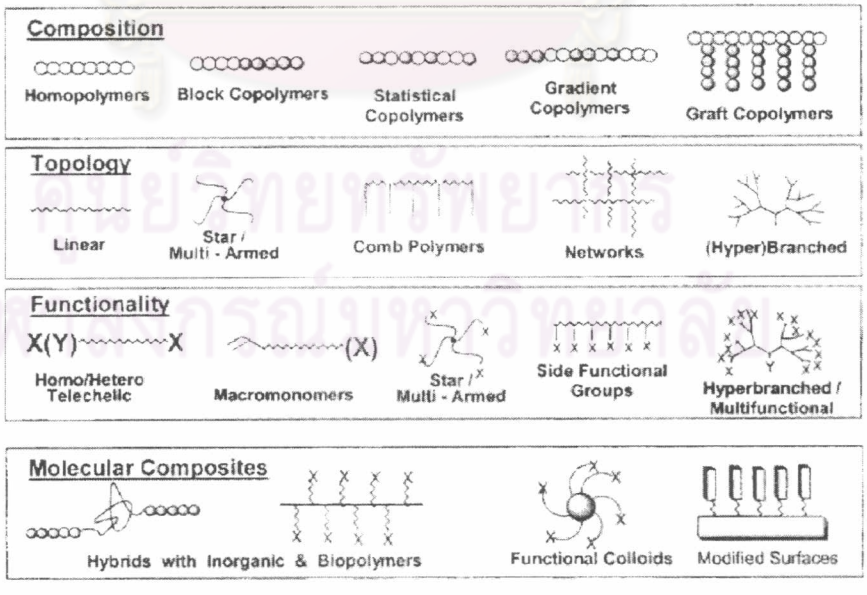

Figure 2.4 Architectural forms of polymers avaiable by living polymerization techniques.

In this research, free radical process for living polymerization is selected and described. The concept of using stable free radicals, such as nitroxides, to reversibly react with the growing polymer radical chain end can be traced back to the pioneering work of Rizzardo and Mozd [16]. After further refinement by Georges [17], the basic blueprint for all subsequent work in the area of "living" free radical polymerization was developed. Subsequently, the groups of Sawamoto[18], Matyjaszewski [19], Percec [20] and others [21-22] have replaced the stable nitroxide free radical with transition metal species to obtain a variety of copper-, nickel-, or ruthenium-mediated "living" free radical systems. These systems were called atom transfer radical polymerization (ATRP). This mechanism is an efficient method for carbon-carbon bond formation in organic synthesis. In some of these reactions, a transition-metal catalyst acts as a carrier of the halogen atom in a reversible redox process (Figure 2.5). Initially, the transition-metal species, M_t^n, abstracts halogen atom X from the organic halide, RX, to form the oxidized species, $M_t^{n+1}X$, and the carbon-centered radical $R^\bullet$. In the subsequent step, the radical $R^\bullet$ participates in an inter- or intramolecular radical addition to alkene, Y, with the formation of the intermediate radical species, $RY^\bullet$. The reaction between $M_t^{n+1}X$ and $RY^\bullet$ results in a target product, RYX, and regenerates the reduced transition-metal species, M_t^n, which further promotes a new redox process. The fast reaction between $RY^\bullet$ and $M_t^{n+1}X$ apparently suppresses biomolecular termination between alkyl radicals and efficiently introduces a halogen functional group X into the final product in good to excellent yields.

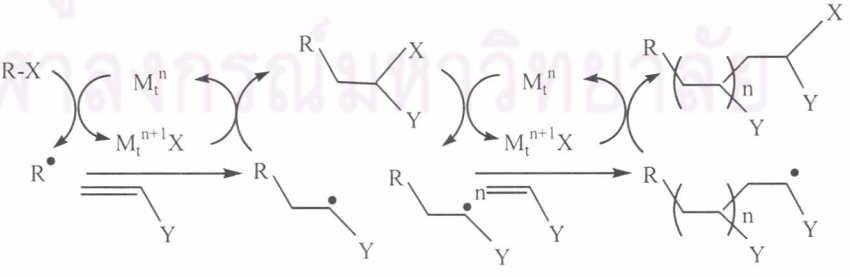

Figure 2.5 The mechanism of ATRP.

The ATRP system relies on one equilibrium reaction in addition to the classical free-radical polymerization scheme (Figure 2.6). In this equilibrium, a dormant species, RX, reacts with the activator, M_t^n, to form a radical $R^\bullet$ and deactivating species, $M_t^{n+1}X$. The activation and deactivation rate parameters are k_{act} and k_{deact}, respectively. Since deactivation of growing radicals is reversible, control over the molecular weight distribution and, in the case of copolymers, over chemical composition can be obtained if the equilibrium meets several requirements [23-24].

1. The equilibrium constant, k_{act}/k_{deact}, must be low in order to maintain a low stationary concentration of radicals. A high value would result in a high stationary radical concentration, and as a result, termination would prevail over reversible deactivation.

2. The dynamics of the equilibrium must be fast; i.e. deactivation must be fast compared to propagation in order to ensure fast interchange of radicals in order to maintain a narrow molecular weight distribution.

$$R\text{-}X + M_t^n \underset{k_{deact}}{\overset{k_{act}}{\rightleftharpoons}} R^\bullet + M_t^{n+1}X$$

Figure 2.6 Equilibrium reaction in ATRP [25].

Futhermore, in 1995, Matyjaszewski has described the use of Cu^IX (X = Br, Cl) with 2,2'-bipyridine (bpy) as a "solubilizing" ligand. The active species has been described as "CuBr·bpy". This system is active toward styrene, acrylates, and methacrylates under the appropriate condition [19]. Percec has also described the role of bpy as partially solubilizing the Cu(I)/Cu(II) catalyst [26]. The role of the bpy is to co-ordinate to Cu(I) to give a *pseudo*-tetrahedral Cu(I) center in solution (Figure 2.7).

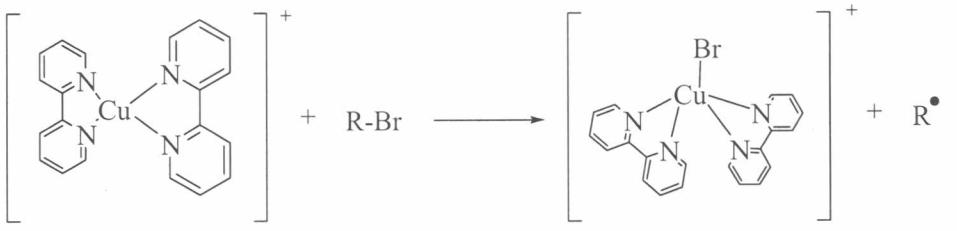

Figure 2.7 The rotation of the bpy ligands from the tetrahedral and co-ordination of halide at the Cu center.

When uncoordinated, bpy exists predominately in the s-trans conformation in the solid state, in solution there is free rotation with the trans conformation and orthogonal rings are preferred over the cis conformation. Metal complexes contain bpy in a cisoid conformation, forming a planar 5-membered chelating ring. The ligand π^* orbitals can accept electron density from the metal thus stabilizing low oxidation states, in particular Cu(I). Abstraction by the $Cu(bpy)_2^+$ cation of halogen atoms from alkyl halides results in oxidation to Cu(II). The pentaco-ordinated species were shown in Figure 2.6 which involves rotation of the bpy ligands from the tetrahedral and co-ordination of halide at the Cu center. This has also been proposed by Matyjaszewski [27]. Thus, if this proposed mechanism is correct, the two main roles of the ligand are (i) stabilization of Cu(I) by removal of electron density from the metal and (ii) the ability to interchange between tetrahedral Cu(I) and distorted square based pyramidal Cu(II). Copper(I) halides are very insoluble in organic solvents and monomers, and therefore the concept of solubilizing copper(I) indeed valid. However, the use of either Cu^IBr or Cu^ICl with bpy under atom transfer radical polymerization conditions results in a very heterogeneous reaction medium with a deep red $Cu\text{-}(bpy)_2$ complex in solution and insoluble copper halide visible as a pale green solid. Under these conditions the actual concentration of active catalyst is impossible to determine. The system has been modified to give a homogeneous system by the use of bipyridines with alkyl substituents in the 4^{th} position e.g. *tert*-butyl [28-29]. The use of these homogeneous copper(I) complexes results in a marked lowering of the polydispersity index (PDI) to approximately 1.05.

In 2003, Matyjaszewski's group studied the effect of [bpy]/[Cu(I)] ratio, polarity of the medium, and nature of alkyl bromides on the activation rate constants (k_{act}) in ATRP. The highest values of k_{act} for Cu(I)Br were obtained at [bpy]/[Cu(I)Br] ~ 2/1 and 1/1 in more polar and less polar solvents, respectively. This was ascribed to different structures of the complex, $Cu(bpy)_2^+Br^-$ and $Cu(bpy)_2^+CuBr_2^-$, correspondingly as shown in Figure 2.8 [30].

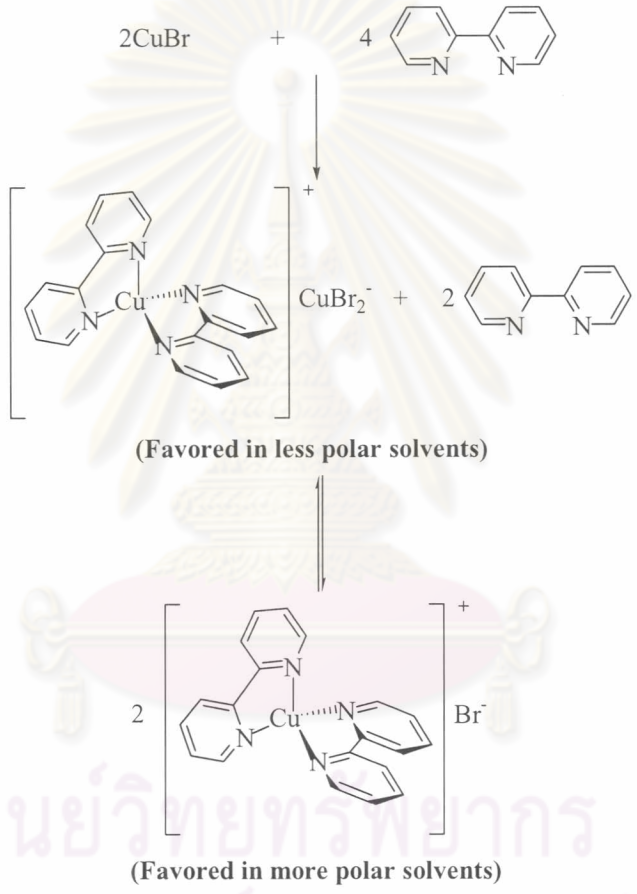

Figure 2.8 Complex formation equilibrium in polar and nonpolar solvents [30].

ATRP can be applied to a large variety of monomers [8-11] to produce polymers with well-defined microstructures [31-34]. The success of ATRP in synthesizing hydrophilic polymer provides an additional advantage over the traditional living ionic polymerization. The first example of aqueous ATRP was from Matyjaszewski's group in 1998. They found that ATRP of 2-hydroxyethyl acrylate (HEA) can be carried out directly in water in the presence of CuX/bpy/R-X

at 90°C. After polymerization for 12 h, 87% monomer conversion was achieved, the molecular weight of the final product was 14,700, and the final polydispersity was 1.34 [35]. Similar results were obtained by Armes's group for the controlled polymerization of sodium methacrylate in water at 90°C. Monomer conversions of 70-80% were achieved after 10 h, with polydispersity of 1.20-1.30 [36]. In 2000, Wang and Armes reported the facile ATRP of methoxy-capped oligo(ethylene glycol) methacrylate (OEGMA) in water at 20°C with various initiators. A remarkably fast rate of polymerization was observed, with unusually high monomer conversions (up to 99%), first-order monomer kinetics, and predetermined molecular weights with narrow molecular weight distributions, indicating good "living" character [37-38]. In 2001, the efficient, controlled polymerization of 2-hydroxyethyl methacrylate (HEMA) is achieved using ATRP in methanol/water mixtures or pure methanol at 20°C by Armes and coworkers [39]. In the same year, Armes's group can polymerize to high conversions of the biocompatible polymers based on 2-methacryloyloxyethyl phosphorylcholine (MPC) in both aqueous and alcoholic media at ambient temperature via ATRP. Low polydispersities were obtained [40-41].

2.3 Polymer Brush

Polymer brushes refer to an assembly of polymer chains which are tethered by one end to a surface or an interface [42]. Tethering is sufficiently dense that the polymer chains are crowded and forced to stretch away from the surface or interface to avoid overlapping, sometimes much further than the typical unstretched size of a chain. These stretched configurations are found under equilibrium conditions; neither a confining geometry nor an external field is required. This situation, in which polymer chains stretch along the direction normal to the grafting surface, is quite different from the typical behavior of flexible polymer chains in solution where chains adopt a random-walk configuration. A series of discoveries show that the deformation of densely tethered chains affects many aspects of their behavior and results in many novel properties of polymer brushes [42].

Polymer brushes are a central model for many practical polymer systems such as polymer micelles, block copolymers at fluid–fluid interfaces (e.g. microemulsions and vesicles), grafted polymers on a solid surface, adsorbed diblock copolymers and graft copolymers at fluid–fluid interfaces. All of these systems, illustrated in Figure 2.9, have a common feature: the polymer chains exhibit deformed configurations. Solvent can be either present or absent in polymer brushes. In the presence of a good solvent, the polymer chains try to avoid contact with each other to maximize contact with solvent molecules. In the absence of a solvent (melt conditions), polymer chains must stretch away from the interface to avoid overfilling incompressible space.

The interface to which polymer chains are tethered in the polymer brushes may be a solid substrate surface or an interface between two liquids, between a liquid and air, or between melts or solutions of homopolymers. Tethering of polymer chains on the surface or interface can be reversible or irreversible. For solid surfaces, the polymer chains can be chemically bonded to the substrate or may be just adsorbed onto the surface. Physisorption on a solid surface is usually achieved by block copolymers with one block interacting strongly with the substrate and another block interacting weakly. For interfaces between fluids, the attachment may be achieved by similar adsorption mechanisms in which one part of the chain prefers one medium and the rest of the chain prefers the other.

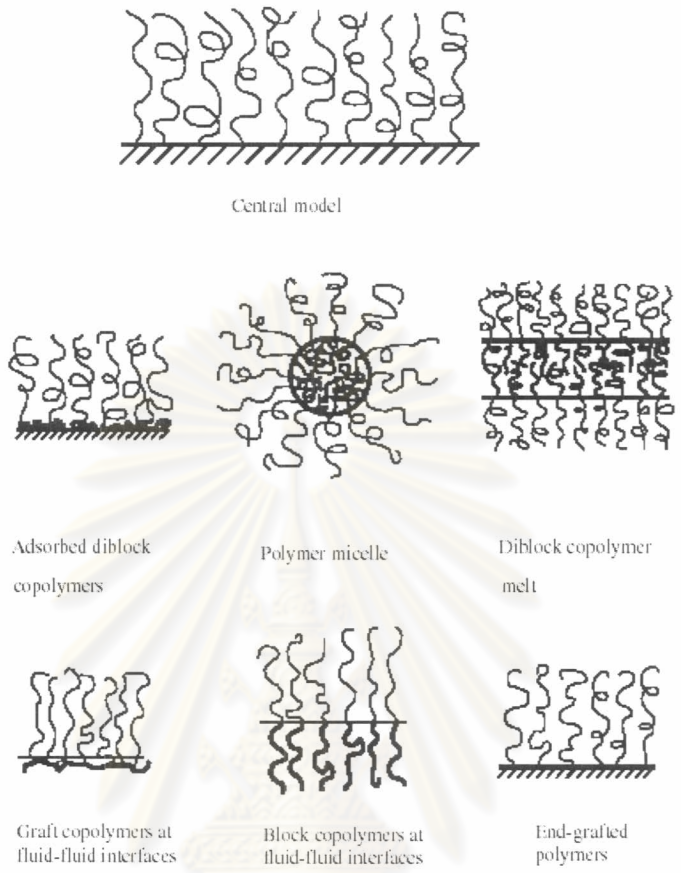

Figure 2.9 Examples of polymer systems comprising polymer brushes.

Polymer brushes (or tethered polymers) attracted attention in 1950s when it was found that grafting polymer molecules to colloidal particles were a very effective way to prevent flocculation [42]. In other words, one can attach polymer chains which prefer the suspension solvent to the colloidal particle surface; the brushes of two approaching particles resist overlapping and colloidal stabilization are achieved. The repulsive force between brushes arises ultimately from the high osmotic pressure inside the brushes. Subsequently it was found that polymer brushes can be useful in other applications such as new adhesive materials [43-44], protein-resistant biosurfaces [45], chromotographic devices [46], lubricants [47], polymer surfactants [42] and polymer compatibilizers [42]. Tethered polymers which possess low critical solution temperature (LCST) properties exhibit different wetting

properties above and below LCST temperature [48]. A very promising field that has been extensively investigated is using polymer brushes as chemical gates. Ito and coworkers [49-51] have reported pH sensitive, photosensitive, oxidoreduction sensitive polymer brushes covalently tethered on porous membranes, which are used to regulate the liquid flowing rate through porous membranes. Suter and coworkers [52-53] have prepared polystyrene brushes on high surface area mica for the fabrication of organic–inorganic hybrids. Cation-bearing peroxide free-radical initiators were attached to mica surfaces via ion exchange and used to polymerize styrene. This process is important in the field of nanocomposites. Patterned thin organic films could be useful in microelectrics [54], cell growth control [55-56], biomimetic material fabrication [57], microreaction vessel and drug delivery [58].

In terms of polymer chemical compositions, polymer brushes tethered on a solid substrate surface can be divided into homopolymer brushes, mixed homopolymer brushes, random copolymer brushes and block copolymer brushes. Homopolymer brushes refer to an assembly of tethered polymer chains consisting of one type of repeat unit. Mixed homopolymer brushes are composed of two or more types of homopolymer chains [59]. Random copolymer brushes refer to an assembly of tethered polymer chains consisting of two different repeat units which are randomly distributed along the polymer chain [60]. Block copolymer brushes refer to an assembly of tethered polymer chains consisting of two or more homopolymer chains covalently connected to each other at one end [61]. Homopolymer brushes can be further divided into neutral polymer brushes and charged polymer brushes. They may also be classified in terms of rigidity of the polymer chain and would include flexible polymer brushes, semiflexible polymer brushes and liquid crystalline polymer brushes. These different polymer brushes are illustrated in Figure 2.10.

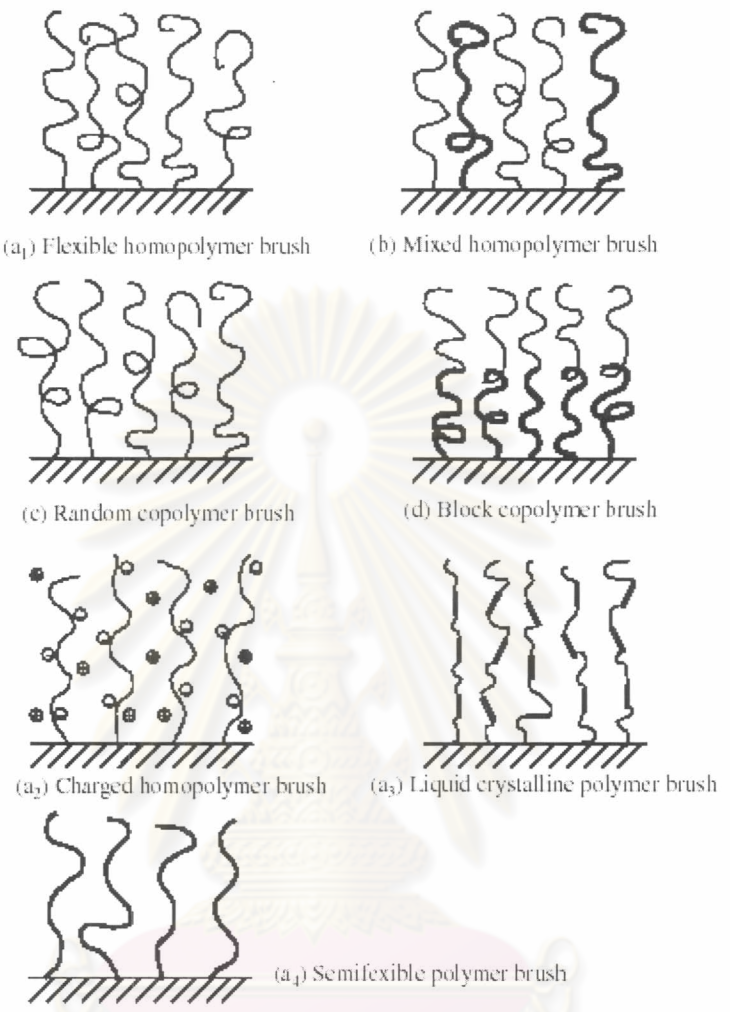

Figure 2.10 Classification of linear polymer brushes, (a_1–a_4) homopolymer brushes; (b) mixed homopolymer brush; (c) random copolymer brush; (d) block copolymer brush.

Generally, there are two ways to fabricate polymer brushes: physisorption and covalent attachment (Figure 2.11). For polymer physisorption, block copolymers adsorb onto a suitable substrate with one block interacting strongly with the surface and the other block interacting weakly with the substrate. The disadvantages of physisorption include thermal and solvolytic instabilities due to the non-covalent nature of the grafting, poor control over polymer chain density and complications in synthesis of suitable block copolymers. Tethering of the polymer chains to the surface is one way to surmount some of these disadvantages. Covalent attachment of

polymer brushes can be accomplished by either "grafting to" or "grafting from" approaches. In a "grafting to" approach, preformed end-functionalized polymer molecules react with an appropriate substrate to form polymer brushes. This technique often leads to low grafting density and low film thickness, as the polymer molecules must diffuse through the existing polymer film to reach the reactive sites on the surface. The steric hindrance for surface attachment increases as the tethered polymer film thickness increases. To overcome this problem, the "grafting from" approach is a more promising method in the synthesis of polymer brushes with a high grafting density. "Grafting from" can be accomplished by treating a substrate with plasma or glow-discharge to generate immobilized initiators onto the substrate followed by in situ surface-initiated polymerization. However "grafting from" well-defined self-assembled monolayers (SAMs) is more attractive due to a high density of initiators on the surface and a well-defined initiation mechanism. Also progress in polymer synthesis techniques makes it possible to produce polymer chains with controllable lengths. Polymerization methods that have been used to synthesize polymer brushes include cationic, anionic, TEMPO-mediated radical, atom transfer radical polymerization (ATRP) and ring opening polymerization.

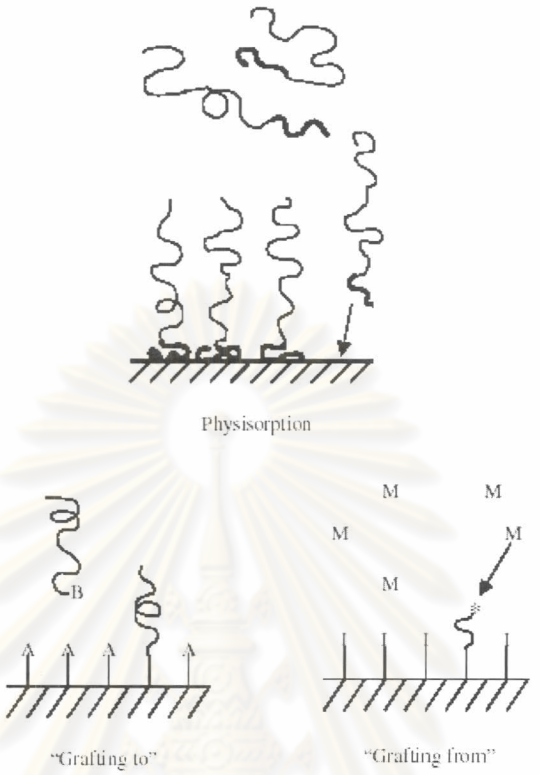

Figure 2.11 Preparation of polymer brushes by "physisorption", "grafting to" and "grafting from".

In order to achieve a better control of molecular weight and molecular weight distribution and to obtain novel polymer brushes like block copolymer brushes, controlled radical polymerizations including ATRP, reverse ATRP, TEMPO-mediated and iniferter radical polymerizations have been used to synthesize tethered polymer brushes on solid substrate surfaces [62-67].

ATRP is a newly developed controlled radical polymerization [28]. It has attracted considerable attention due to its control of molecular weight, molecular weight distribution and synthesis of block copolymers. Husseman and coworkers [64] applied ATRP in the synthesis of tethered polymer brushes on silicon wafers and achieved great success. They prepared SAMs of 5-trichlorosilylpentyl-2-bromo-2-methylpropionate on silicate substrates. The α-bromoester is a good initiator for ATRP. They have successfully synthesized PMMA brushes by the polymerization of MMA initiated from the SAMs. It has also been reported that tethered

polyacrylamide has been obtained from surface initiated ATRP of acrylamide on a porous silica gel surface [65].

Recently, Matyjaszewski and coworkers [68] reported a detailed study of polymer brush synthesis using ATRP in controlled growth of homopolymer and block copolymers from silicon surfaces. They described that the persistent radical effect must be considered in controlled radical polymerizations. In other words, a sufficient concentration of deactivation must be available to provide control over chain lengths and distributions. The Cu (II) can be supplied by termination of initiator molecules in the early stages of the polymerization or by addition of the transition metal complex prior to commencement of the reaction. Moreover, the only factor affected is the kinetics of the reaction; in the former case, first-order consumption of monomer is dictated by the chains generated from the free initiator while in the latter, due to the extremely low concentration of alkyl halide bound to the surface and low monomer conversion, growth of polymer chains scales linearly with reaction time. Their conclusion suggested that the design of such complex structures whether in solution or at an interface, understanding of the relative rates of chain propagation, equilibrium constants, and the influences of the end group, metal, and ligand in crossover reaction are important. Factors such as initiator functionality and blocking efficiency can have a profound influence on the physical properties of the resulting material.

In 2001, Armes and coworkers synthesized polymer brush by ATRP of 2-hydroxyethyl methacrylate (HEMA) and methoxy-capped oligo(ethylene glycol) methacrylate (OEGMA) from silica modified with an initiator layer composed of 2-bromoisobutylrate. These polymer-grafted silica particles produced in this initial study are fascinating new "model" sterically stabilized colloids which are likely to prove attractive for both theoretical and experimental studies. The aqueous solution properties of the grafted polymer chains determine the colloid stability of the particles, as expected [69].

In the same year, *von* Werne and Patten [70] reported the preparation of structurally well-defined polymer-nanoparticle hybrids by modifying the surface of

silica nanoparticles with initiatiors for ATRP by using these initiator-modified nanoparticles as macroinitiators. They found that polymerizations of styrene and methyl methacrylate (MMA) using the nanoparticle initiators displayed the diagnostic criteria for a controlled / "living" radical polymerization: an increase in the molecular weight of the pendant polymer chains with monomer conversion and a narrow molecular weight distribution for the grafted chains. Polymerization of styrene from smaller silica nanoparticles (75-nm-diameter) exhibited good molecular weight control, while polymerization of MMA from the same nanoparticles exhibited good molecular weight control only when a small amount of free initiator was added to the polymerization solution. For the polymerizaiton of both styrene and MMA from larger silica nanoparticles (300-nm-diameter) did not exhibit molecular weight control. Molecular weight control was induced by the addition of a small amount of free initiator to the polymerization but was not induced when 5-15 mol% of deactivator (Cu(II) complex) was added. These findings provide guidance for efforts in using ATRP for the controlled grafting of polymers from high and low surface area substrates.

In 2004, Feng et al. [71] prepared poly(2-methacryloyloxyethyl phosphorylchloline) (PMPC) layers on silicon wafer surfces by combining an initiator self-assembled monolayer technique with ATRP grafting. They used two methods to control the grafting process. One was to add free initiator to the reaction system; the other was to add excess deactivator. This process indicated the surface thickness increased linearly with MPC conversion. The thickness depended on catalyst and monomer concentrations, as well as activator/deactivator ratio. Increasing the ratio of $CuBr_2$/CuBr (activator/deactivator) decreased radical termination which led to better control over the growth of the polymer chains; however, it also decreased the polymerization rate. Increasing the ratio of monomer/catalyst and monomer concentration also increased the polymer layer thickness.

The conformation of polymer end-grafted on a solid surface is an importance parameter, it plays an important surface property in many areas of science and technology, e.g., colloid stabilization, adhesion, lubrication, tribology, and rheology.

The conformation of those polymers in good solvent can dramatically change with graft density; at low graft density, a "mushroom" structure will be formed with the coil dimension similar to that of ungrafted chains. With increasing graft density, graft chains will be obliged to stretch away from the surface. For example, in 2002, Jones and coworkers [72] studied the influence of initiator density on the controlled growth of polymer brushes in aqueous solution at room temperature. They used mixed monolayers comprising of undecanethiol and ω–mercaptoundecyl bromoisobutyrate (active initiator) to initiate the controlled radical polymerization of MMA from gold. They found an almost linear relatonship between initiator density and the growth rate of the polymer brush formed. SAMs composed of 10% and 50% of active initiator grow PMMA brushes ~ 1/10 and ½ the thickness of polymer brushes grafted from SAMs comprising 100% of active initiator. However, they did not find a maximum initiator density, beyond which no further incrase in polymer thickness was observed. For morphology of polymer brush could be observed between the different initiator concentrations. The lower active initiator brushes showed fairly large and polydisperse grains due to the polymer chains were growing very far apart, coalescing into large grains. While increasing active initiator surface exhibited the smaller grainlike structures, fairly monodisperse and densily packed. When increasing initiator density to 100% active initiator resulted in almost featureless films (shown in Figure 2.12)

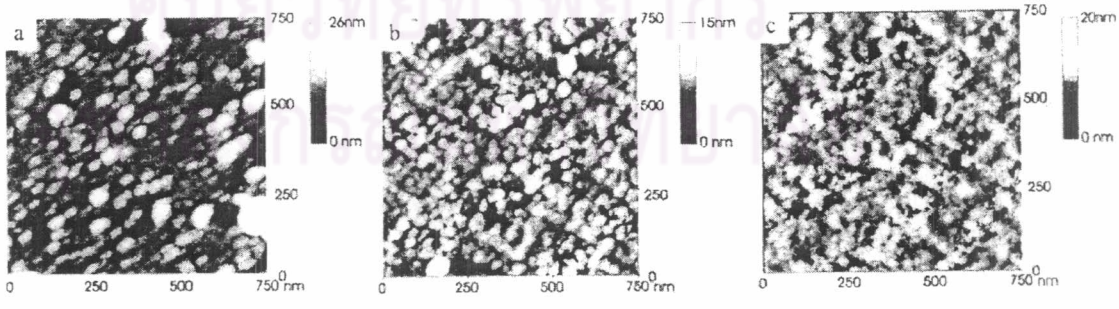

Figure 2.12 AFM images of PMMA brushes grown from gold evaporated onto mica after 50 min of reaction time: (a) 10% of active initiator, (b) 25% of active initiator and (c) 100% of active initiator

Yu, et al. [73] reported that the controlled grafting of well-defined polymer brushes of poly(methyl methacrylate) (PMMA) was carried out via ATRP on the hydrogen-terminated Si surfaces (Si-H surface). Prior to the surface initiated ATRP, the Si-H surface was functionalized by the α–bromoester group in 3 steps: (i) coupling of an ω–unsaturated alkyl ester with the Si-H surface under UV irradiation, (ii) reduction of the ester group by $LiAlH_4$, and (iii) esterification of the surface-tethered hydroxyl group with 2-bromoisobutylate bromide. XPS and ellipsometry data indicated the formation of polymer brushes on the silicon surface. Kinetic studies revealed a linear increase in thickness of the surface graft polymerized film with reaction time and $\overline{M}_n$ of the homopolymer in solution, indicating that the chain growth from the surface was a controlled process with a "living" characateristic. AFM images suggested that the ATRP graft polymerization has proceeded uniformly on the Si-R_3Br surface to give rise to a dense coverage of PMMA on the silicon surface. As shown in Figure 2.13c, the grafted PMMA chains on the silicon surface exist as a distinctive overlayer. The formation of the nanosized islands probably has resulted from the nanoscaled phase aggregation of the grafted polymer after the surface has been dried.

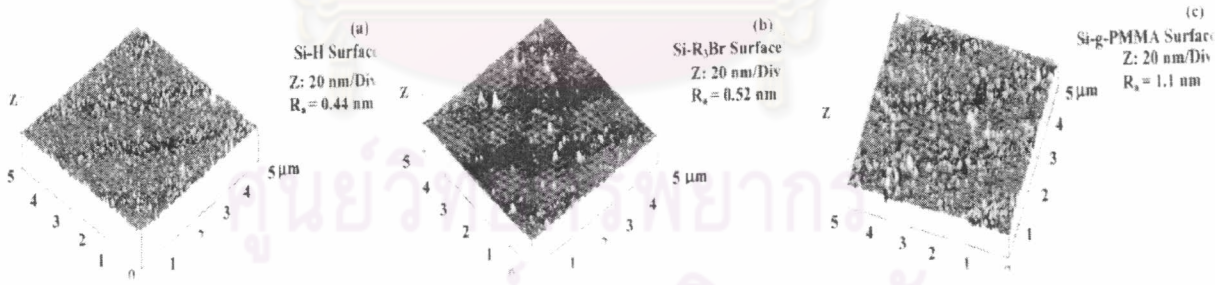

Figure 2.13 AFM images of (a) Si-H surface, (b) Si- R_3Br surface, and (c) Si-*g*-PMMA surface

2.4 Characterization Techniques

2.4.1 Ellipsometry [74]

Ellipsometry is a sensitive optical technique for determining properties of surfaces and thin films. If linearly polarized light of a known orientation is reflected at oblique incidence from a surface then the reflected light is elliptically polarized. The shape and orientation of the ellipse depend on the angle of incidence, the direction of the polarization of the incident light, and the reflection properties of the surface. Ellipsometry measures the polarization of the reflected light with a quarter-wave plate followed by an analyzer; the orientations of the quarter-wave plate and the analyzer are varied until no light passes though the analyzer. From these orientations and the direction of polarization of incident light are expressed as the relative phase change, Δ, and the relative amplitude change, Ψ, introduced by reflection from the surface. These values are related to the ratio of Fresnel reflection coefficients, R_p and R_s for p and s- polarized light, respectively.

$$\mathrm{Tan}(\Psi)\, e^{i\Delta} = \frac{R_p}{R_s} \qquad (2.2)$$

An ellipsomer measures the changes in the polarization state of light when it is reflected from a sample. If the sample undergoes a change, for example, a thin film on the surface changes its thickness, then its reflection properties is also changed. Measuring these changes in the reflection properties allow us to deduce the actual change in the film's thickness.

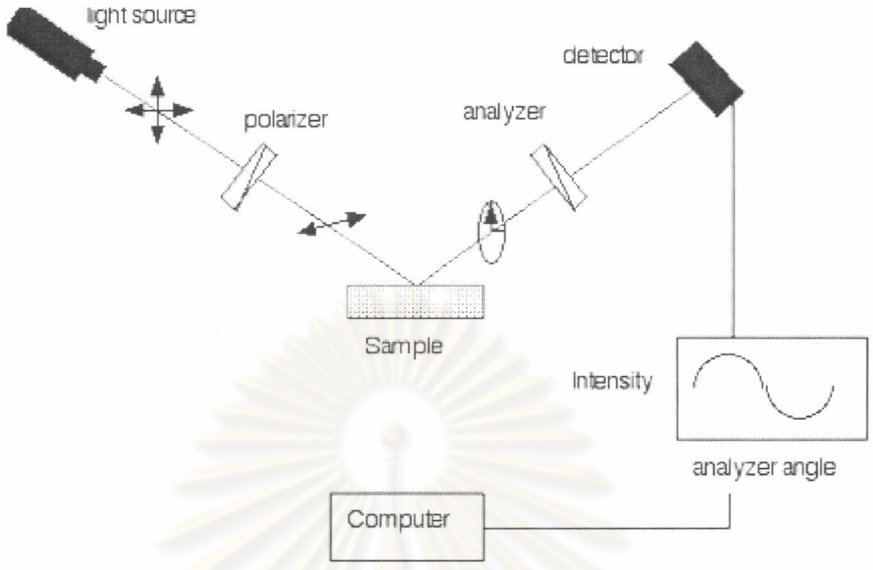

Figure 2.14 Schematic diagram of the geometry of an ellipsometry experiment

2.4.2 Contact Angle Measurement [75]

Contact angle measurements are often used to assess changes in the wetting characteristics of a surface and hence indicate a change in surface energy. The technique is based on the three-phase boundary equilibrium described by Young's equation.

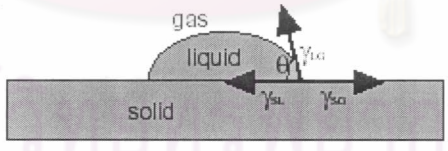

Figure 2.15 Schematic representation of the Young's equation.

$$\gamma_{LG}\cos\theta = \gamma_{SG} - \gamma_{SL} \qquad (2.3)$$

where γ_{LG}, γ_{SG} and γ_{SL} are the interfacial tension between the phases with subscripts L, G, S corresponding to liquid, gas, and solid phase respectively and θ refers to the equilibrium contact angle. The Young's equation applies for a perfectly

homogeneous atomically flat and rigid surface and therefore supposes many simplifications. In the case of real surfaces, the contact angle value is affected by surface roughness, heterogeneity, vapor spreading pressure, and chemical contamination of the wetting liquid. Although the technique to measure contact angles is easy, data interpretation is not straightforward and the nature of different contributions to the surface is a matter of discussion. Generally, we can define the complete wetting, wetting, partial wetting, and nonwetting according to Figure 2.16.

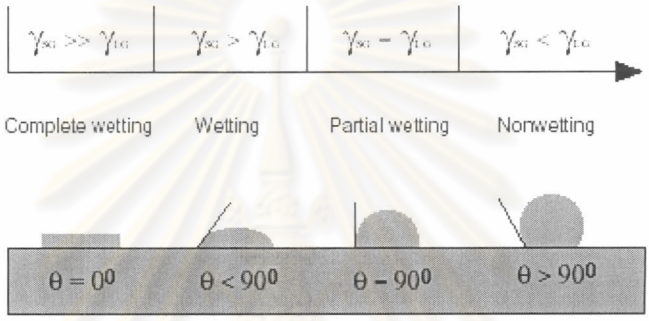

Figure 2.16 Schematic representation of wettability.

2.4.3 X-ray Photoelectron Spectroscopy (XPS) [75]

XPS is an abbreviation for X-ray Photoelectron Spectroscopy. Another name is ESCA which is an acronym for Electron Spectroscopy for Chemical Analysis. In XPS or ESCA, a beam of (monochromatic) X-rays is first produced by electron bombardment of an anode material (Al, Mg, Si). When the X-rays interact with the sample under investigation, they can ionize electrons that are in core levels (such as 1s, 2s, etc.). If the binding energy of the electron in the core hole was EB, then the kinetic energy of the electron ejected from the surface can be given in the energy diagram (Figure 2.17).

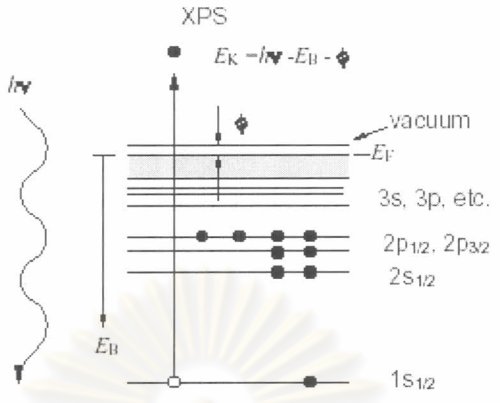

Figure 2.17 Schematic diagram of the X-ray photoelectron emission process.

$$E_K = h - E_B - \phi \qquad (2.4)$$

where E_K is the measured electron kinetic energy, $h\upsilon$ the energy of the exciting radiation, E_B the binding energy of the electron in the solid, and ϕ the spectrometer work function. Since $h\upsilon$ is a well-defined quantity, the electron binding energies can be calculated by measuring the kinetic energies of the electrons that are ejected from the sample, using the above equation. The electron energies are measured using an electrostatic energy analyzer such as a "hemispherical analyzer". The analyzer measures the kinetic energy distribution of the emitted electrons. A general schematic drawing of the main components of the XPS instrument is shown in Figure 2.18. The main components of the system include the vacuum system, the x-ray source, the sample stage, and the analyzer. The energy discrimination of the electrons is obtained by sweeping the potential(s) in the lens or by using a grid system in front of the analyzer. The sensitivity of the instrument is dependent on the X-ray source used, the analyzed area, geometrical factors and the efficiencies of the lens, the analyzer and the detector. The energy resolution is due to the inherent width of the X-ray radiation and the resolving power of the spectrometer.

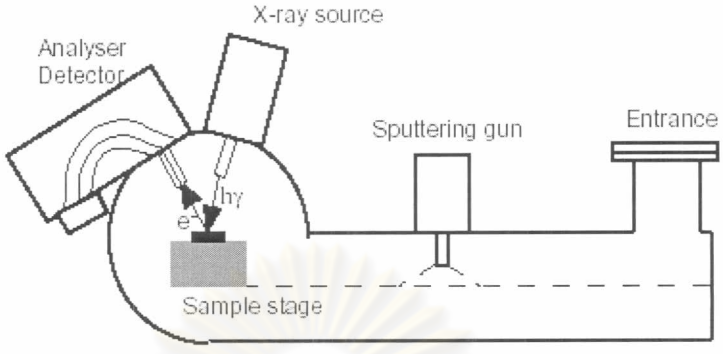

Figure 2.18 General schematic drawing of the XPS instrument.

XPS can provide the following information:

1. Elemental identification. Because the number of protons increases as we progress through the periodic table, the electron binding energies for a fixed core level (such as the 1s level) will increase monotonically; thus, measuring the electron kinetic energy is equivalent to determining which elements are present on the surface.

2. Oxidation states for any given elements. There will be small shifts in the binding energies due to changes in oxidation states; higher oxidation states generally have higher binding energies, and emit electrons with lower kinetic energies.

3. Quantitative analyses through curve fitting and calculation of atomic concentrations because the photoelectron intensity is directly related to the atomic concentrations of the photoemitting atoms.

4. Depth profiling when combined with ion etching (sputtering) techniques.

5. Images or maps showing the distribution of the elements or their chemical states over the surface. Modern instruments can have a spatial resolution down to a few microns.

2.4.4 Atomic force Microscopy (AFM) [76]

AFM is a type of scanning probe microscopy, allowing three-dimensional topographical imaging of surface. The AFM probe is in physical contact with the

surface as it moves over the sample. Because it may be used on any surface, AFM is much more suited to polymer surface analysis. The essential features of AFM are shown in Figure 2.19. The tip of the probe, which is commonly made of silicon nitride, is attached to a cantilever bearing a reflective surface upon which is a laser beam is directed. The sample is mounted on a piezoelectric support, which moves in response to surface variations sensed by the probe. As the tip is scanned (or "rastered") over the surface, topological variations cause deflections in the cantilever that are monitored by recording the path of the reflected laser beam. A computer interprets the deflections as a three-dimensional profile of the polymer surface with resolution in the angstrom range, which is several orders of magnitude better than that obtained by SEM.

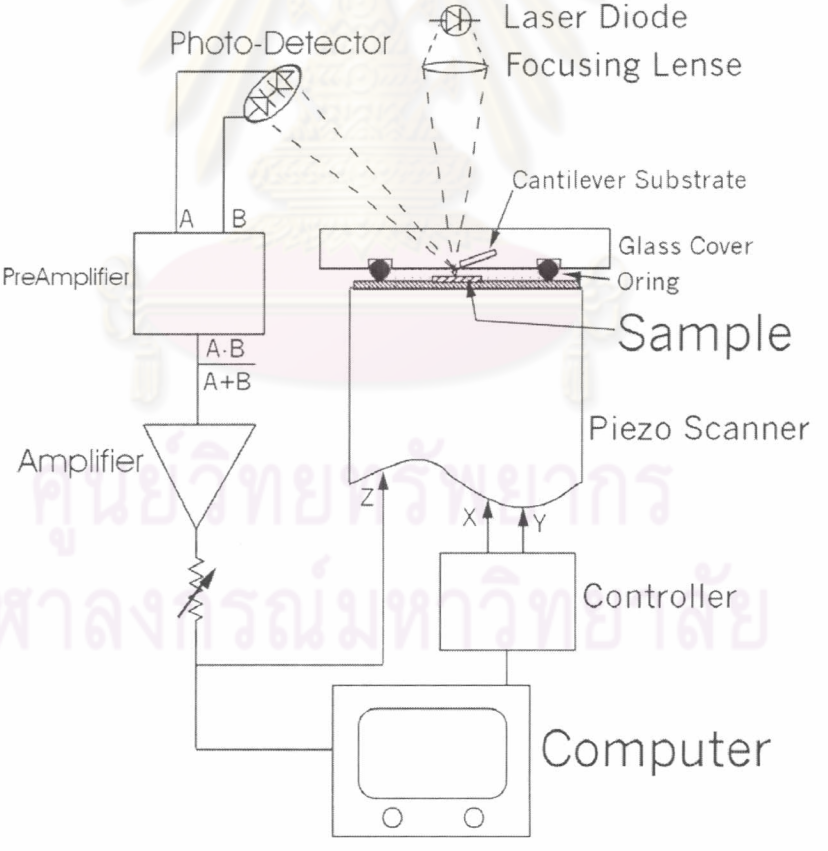

Figure 2.19 Schematic diagram of an atomic force microscope.

The Atomic Force Microscope (AFM) is being used to solve processing and materials problems in a wide range of technologies affecting the electronics, telecommunications, biological, chemical, automotive, aerospace, and energy industries. The materials being investigating include thin and thick film coatings, ceramics, composites, glasses, synthetic and biological membranes, metals, polymers, and semiconductors. The AFM is being applied to studies of phenomena such as abrasion, adhesion, cleaning, corrosion, etching, friction, lubrication, plating, and polishing. By using AFM one cannot only image the surface in atomic resolution but also measure the force at nano-newton scale. The publications related to the AFM are growing speedily since its birth.

The first AFM was made by meticulously gluing a tiny shard of diamond onto one end of a tiny strip of gold foil. In 1985 Binnig and Gerber used the cantilever to examine insulating surfaces. A small hook at the end of the cantilever was pressed against the surface while the sample was scanned beneath the tip. The force between tip and sample was measured by tracking the deflection of the cantilever. This was done by monitoring the tunneling current to a second tip positioned above the cantilever. They could delineate lateral features as small as 300 Å. The force microscope emerged in this way. In fact, without the breakthrough in tip manufacture, the AFM probably would have remained a curiosity in many research groups. It was Albrecht, a fresh graduate student, who fabricated the first silicon microcantilever and measured the atomic structure of boron nitride. Today the tip-cantilever assembly typically is microfabricated from Si or Si_3N_4. The era of AFM came finally when the Zurich group released the image of a silicon (111) 7X7 pattern. The world of surface science knew that a new tool for surface microscope was at hand. After several years the microcantilevers have been perfected, and the instrument has been embraced by scientists and technologists.

The force between the tip and the sample surface is very small, usually less than 10^{-9} N. How to monitor such small forces is another story. The detection system does not measure force directly. It senses the deflection of the microcantilever. The detecting systems for monitoring the deflection fall into several categories. The first device introduced by Binnig was a tunneling tip placed above the metallized surface

of the cantilever. This is a sensitive system where a change in spacing of 1 Å between tip and cantilever changes the tunneling current by an order of magnitude. It is straightforward to measure deflections smaller than 0.01 Å. Subsequent systems were based on the optical techniques. The interferometer is the most sensitive of the optical methods, but it is somewhat more complicated than the beam-bounce method which was introduced by Meyer and Amer. The beam-bounce method is now widely used as a result of the excellent work by Alexander and colleagues. In this system an optical beam is reflected from the mirrored surface on the back side of the cantilever onto a position-sensitive photodetector. In this arrangement a small deflection of the cantilever will tilt the reflected beam and change the position of beam on the photodetector. A third optical system introduced by Sarid uses the cantilever as one of the mirrors in the cavity of a diode laser. Motion of the cantilever has a strong effect on the laser output, and this is exploited as a motion detector

The principles on how the AFM works are very simple. An atomically sharp tip is scanned over a surface with feedback mechanisms that enable the piezo-electric scanners to maintain the tip at a constant force (to obtain height information), or height (to obtain force information) above the sample surface. Tips are typically made from Si_3N_4 or Si, and extended down from the end of a cantilever. The nanoscope AFM head employs an optical detection system in which the tip is attached to the underside of a reflective cantilever. A diode laser is focused onto the back of a reflective cantilever. As the tip scans the surface of the sample, moving up and down with the contour of the surface, the laser beam is deflected off the attached cantilever into a dual element photodiode. The photodetector measures the difference in light intensities between the upper and lower photodetectors, and then converts to voltage. Feedback from the photodiode difference signal, through software control from the computer, enables the tip to maintain either a constant force or constant height above the sample. In the constant force mode, the piezo-electric transducer monitors real time height deviation. In the constant height mode, the deflection force on the sample is recorded. The latter mode of operation requires calibration parameters of the scanning tip to be inserted in the sensitivity of the AFM head during force calibration of the microscope.

Some AFM's can accept full 200 mm wafers. The primary purpose of these instruments is to quantitatively measure surface roughness with a nominal 5 nm lateral and 0.01nm vertical resolution on all types of samples. Depending on the AFM design, scanners are used to translate either the sample under the cantilever or the cantilever over the sample. By scanning in either way, the local height of the sample is measured. Three dimensional topographical maps of the surface are then constructed by plotting the local sample height versus horizontal probe tip position.

The concept of resolution in AFM is different from radiation based microscopies because AFM imaging is a three dimensional imaging technique. The ability to distinguish two separate points on an image is the standard by which lateral resolution is usually defined. There is clearly an important distinction between images resolved by wave optics and scanning probe techniques. The former is limited by diffraction, and later primarily by apical probe geometry and sample geometry. Indeed, many authors have seen that it is the radius of curvature that significantly influences the resolving ability of the AFM. Even greater improvements in resolution have been attained with Tapping mode but contact imaging still is capable of high resolution imaging. The brief discussion on resolution was published by Keller

In order to obtain good AFM results, the vibration isolation platform is needed. The vibration isolation consists of a large mass attached to bungy cords firmly anchored to the building. Damping of the oscillation is believed to result from rubbing of the rubber fibres inside of the bungy cord against the outside lining material. Between the low resonance frequency of the bungy cord system and the high resonance frequency of the microscope hardware itself (>10 kHz), the AFM effectively comprises a band pass filter. This allows the microscopists to safely image their samples in the intermediate range of about 1-100 Hz and obtain atomic resolution.

Gel permeation chromatography is extremely valuable for both analytic and preparative work with a wide variety of systems ranging from low to very high molecular weights. The method can be applied to a wide variety of solvents and polymers, depending on the type of gel used. With polystyrene gels, relatively nonpolar polymers can be measured in solvents such as tetrahydrofuran, toluene, or (at high temperatures) *o*-dichlorobenzene; with porous glass gels, more polar systems, including aqueous solvents, can be used. A few milligrams of sample suffices for analytic work, and the determination is complete in as short a time as a few minutes using modern high-pressure, high-speed equipment.

The results of careful gel permeation chromatography experiments for molecular-weight distribution agree so well with results from other techniques that there is serious doubt as to which is correct when residual discrepancies occur.

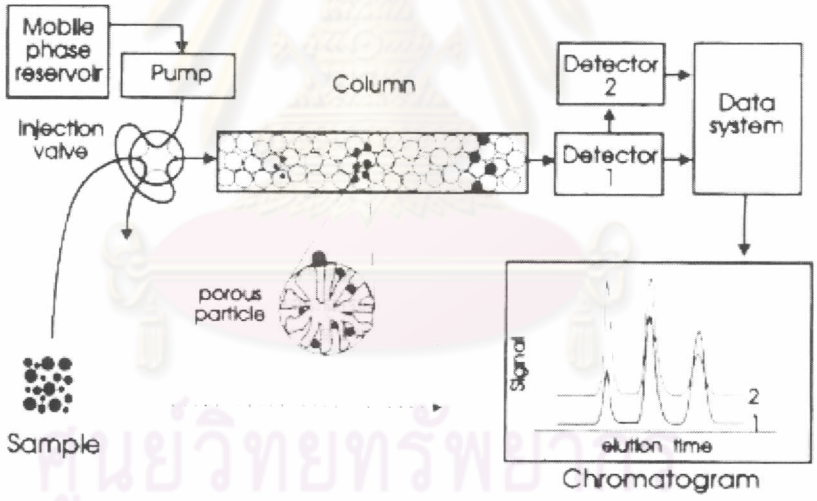

Figure 2.20 Schematic representation of the gel permeation chromatography.